iScience

CellPress
OPEN ACCESS

Article

Controlling radiative heat flows in interior spaces to improve heating and cooling efficiency

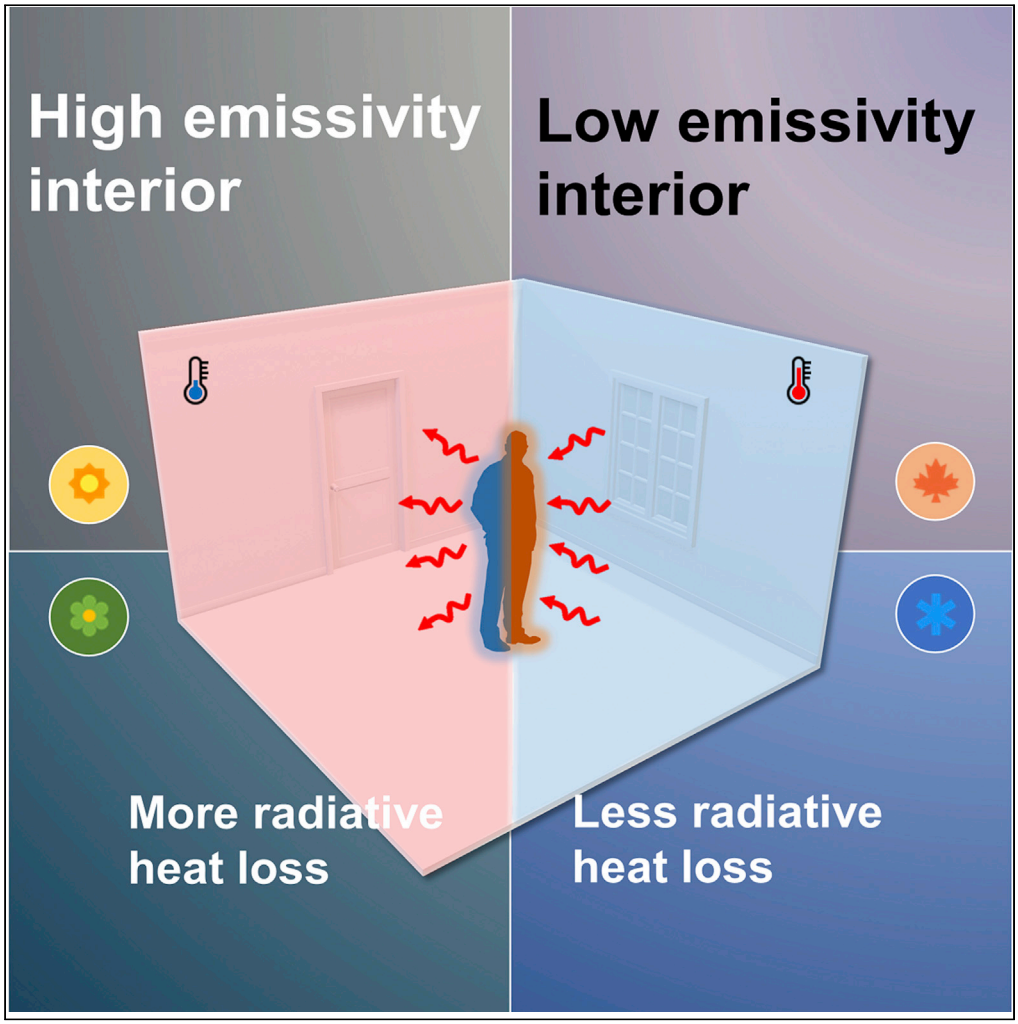

Jin Xu, Aaswath P. Raman

aaswath@ucla.edu

Highlights

Untapped opportunity to control radiative heat transfer for human thermal comfort

Low-emissivity interior surfaces can reduce the heating setpoint by 6.5°C

High emissivity interior surfaces enable a 4.5°C higher cooling setpoint

Tunable emissivity materials maximize year around energy savings

Xu & Raman, iScience *24*, 102825
August 20, 2021
https://doi.org/10.1016/j.isci.2021.102825

iScience

CellPress
OPEN ACCESS

Article

Controlling radiative heat flows in interior spaces to improve heating and cooling efficiency

Jin Xu[1] and Aaswath P. Raman[1,2,*]

SUMMARY

Heating and cooling in buildings account for nearly 20% of energy use globally. The goal of heating and cooling systems is to maintain the thermal comfort of a building's human occupants, typically by keeping the interior air temperature at a setpoint. However, if one could maintain the occupant's thermal comfort while changing the setpoint, large energy savings are possible. Here we propose a mechanism to achieve these savings by dynamically tuning the thermal emissivity of interior building surfaces, thereby decoupling the mean radiant temperature from actual temperatures of interior surfaces. We show that, in cold weather, setting the emissivity of interior surfaces to a low value (0.1) can decrease the setpoint as much as 6.5°C from a baseline of 23°C. Conversely, in warm weather, low-emissivity interior surfaces result in a 4.5°C cooling setpoint decrease relative to high emissivity (0.9) surfaces, highlighting the need for tunable emissivity for maximal year-round efficiency.

INTRODUCTION

Energy consumption in residential and commercial buildings contributes to 30% of total greenhouse gas emissions worldwide (Kingma and van Marken Lichtenbelt, 2015). In the United States, the buildings sector accounts for 41% of primary energy consumption, of which heating and cooling alone is responsible for over 35% (Pérez-Lombard et al., 2008). Heating in particular poses a profound challenge for broader decarbonization goals in temperate and cool climates (The heat is on, 2016). With energy consumption for heating and cooling expected to grow dramatically worldwide in coming decades (Ürge-Vorsatz et al., 2015), improving the efficiency of these systems is a key part of mitigating climate change this century.

The goal of heating and cooling in buildings with human occupants is to maintain their thermal comfort (FANGER, 1970). Thermal comfort is both a quantitative and qualitative judgment that connects an individual's physiological and emotional perceptions of being in a thermally comfortable state (FANGER, 1970; Hensen, 1990). Although thermal comfort is typically assumed to be directly linked to the air temperature set point in a conditioned space, a human occupant's perception of comfort is subject to a range of other factors. These include material properties, metabolic heat production, heat transfer coefficients, and radiative heat losses to external surfaces (Cheng et al., 2013; Moon et al., 2016). Human skin temperature is typically 33°C (Liu et al., 2011, 2013) in comfortable conditions, while the average heat generation rate of a standing adult is 70 W/m^2 (ANSI/ASHRAE, 2017; Okamoto et al., 2017). Previous work has examined how temperature, air velocity, and humidity affect thermal comfort (Yang et al., 2014; Rupp et al., 2015; Coutts et al., 2016). Given the complex array of factors that influence the perception of comfort, and the pressing need for reducing energy use for heating and cooling, it is intriguing to note that an increase in the set point temperature for cooling, or a decrease in the set point for heating, by just 4°C can reduce energy use by up to 45% and 35%, respectively (Hoyt et al., 2005).

In an indoor environment, where most people stay in a sedentary state, more than 50% of the heat generated by the human body is released through thermal radiation in the long-wave infrared part of the spectrum (Arslanoglu and Yigit, 2016). A recent experimental study used a membrane-assisted radiant cooling system to show that radiation and convection can be separated for comfort conditioning and, relying on radiation alone, thermal comfort can be maintained based on existing metrics even in unusually high ambient air conditions (Teitelbaum et al., 2020). Radiative heat transfer between human occupants and

[1]Department of Materials Science and Engineering, UCLA, Los Angeles, CA 90024, USA

[2]Lead contact

*Correspondence: aaswath@ucla.edu

https://doi.org/10.1016/j.isci.2021.102825

their environment largely depends on the radiative properties of clothing, the walls, and other surroundings. Although significant progress has been made on insulation materials for walls, prior studies have primarily examined thermal conductivity, specific heat capacity, and density (Schiavoni et al., 2016; Wang et al., 2018; Dickson and Pavía, 2021).The effect of radiative heat transfer on thermal comfort has also been explored (Winslow et al., 1939; Cai et al., 2017) but remains a comparatively untapped mechanism for efficiency gains. One approach that has attracted considerable interest in recent years is tuning the radiative properties of clothing through photonic and materials-based strategies, making the clothing fabric more or less transparent to thermal radiation emitted from the human wearer, depending on weather conditions (Hsu et al., 2015, 2016; Tong et al., 2015; Guo et al., 2016; Cai et al., 2019; Qiu et al., 2019; Yue et al., 2019; Zhou et al., 2019). Although this approach is conceptually attractive, it poses practical challenges, as it requires the human occupants of a conditioned space to wear specialized clothing depending on weather conditions. Thus, it is more practical to tune the radiative properties of the interior surroundings than to seek to alter the dressing habits of people who happen to be present in a particular building. In winter months, it has previously been noted that having a low-emissivity wall could reduce the heat loss of a radiator in a room with no human occupant (Robinson, 2016). However, to the best of our knowledge, no study has examined how changing the long-wave infrared radiative properties of interior surfaces could reduce energy use for heating and cooling, while maintaining the same thermal comfort level for human occupants. Here we propose and evaluate an untapped approach that seeks to make the environment *surrounding* the human occupants responsive to their radiative heat flows, to enable dramatically improved heating and cooling efficiency.

In cold weather conditions, lower radiative heat loss from the human occupant is desirable, as the air temperature could then be maintained at a lower temperature for the same level of thermal comfort. In these conditions it would thus be preferable to have low-emissivity (high reflectivity) materials in the floor, ceiling, and walls surrounding an occupant. By contrast, in summer or warm weather conditions, the heat generated by a human should be dissipated to interior surfaces, as these surfaces are typically colder than the clothing surface temperature. Thus, high-emissivity (and low-reflectivity) materials in the surroundings would be desirable. The desired radiative properties changing dramatically from low to high emissivity depending on weather conditions and the heat load will necessitate a different approach to enable maximal heating and cooling efficiency year round. On the other hand, a small body of work over the past two decades has identified materials whose emissivity can be tuned in the long-wave infrared part of the spectrum relevant to room temperature blackbody radiation, including by electrochromic control (Mulford et al., 2019; Zhang et al., 2019b). Most encouragingly, recent progress has yielded the first metal-free flexible IR electrochromic devices, based on conducting polymers that act as both the electrochromic material and electrodes (Brooke et al., 2017; Zhang et al., 2019a; Xu et al., 2019), with good emissivity contrast, fast switching, and durability demonstrated. Given these promising materials capabilities, here we investigate the concept of tunable emissivity surfaces for interior spaces in the built environment.

To evaluate the possible set point change and thus energy savings, we implemented computational fluid dynamics (CFD) simulations of an office environment with human occupants. In the simulations, we assume the emissivity of the inner walls can be tuned from that of a near blackbody to a very low value. We show that, in cold weather conditions, a decrease in the set point of 6.5°C is achievable if low-emissivity (0.1) surfaces are used, relative to a baseline set point of 23°C when using conventional materials with a high emissivity (0.9). When multiple occupants are in the conditioned space a decrease of 8.2°C in the set point is possible. Conversely, in hot weather conditions, we show that a decrease in the set point of 2.3°C relative to a typical room set point of 26°C occurs if a low-emissivity surface is used, highlighting the need for tunable emissivity surfaces. Following the CFD simulations, we conducted a detailed thermal comfort analysis for six different wall temperature scenarios. The mean radiant temperature changes when we tune the emissivity of the walls, enabling lower or higher set points for heating and cooling, respectively. A predicted mean vote (PMV) index further indicates that the set point change will not compromise the thermal comfort of human occupants in all six scenarios. We extended our analysis to the building scale by using EnergyPlus (Kant et al., 2018; Shen et al., 2019; Yu et al., 2019) to evaluate the impact of the changed setpoints made possible by tunable emissivity surfaces on energy use on a typical summer and winter day in a temperate climate. In our preliminary analysis, we estimated that the lower setpoints made possible by low-emissivity interior surfaces in cold weather conditions can result in up to 36.8% (in Minneapolis, USA) and 34.1% (in Ancona, Italy) heating energy savings relative to conventional materials. In warm weather conditions, however, low-emissivity interior surfaces are no longer appropriate and would result in a 34.7% (in

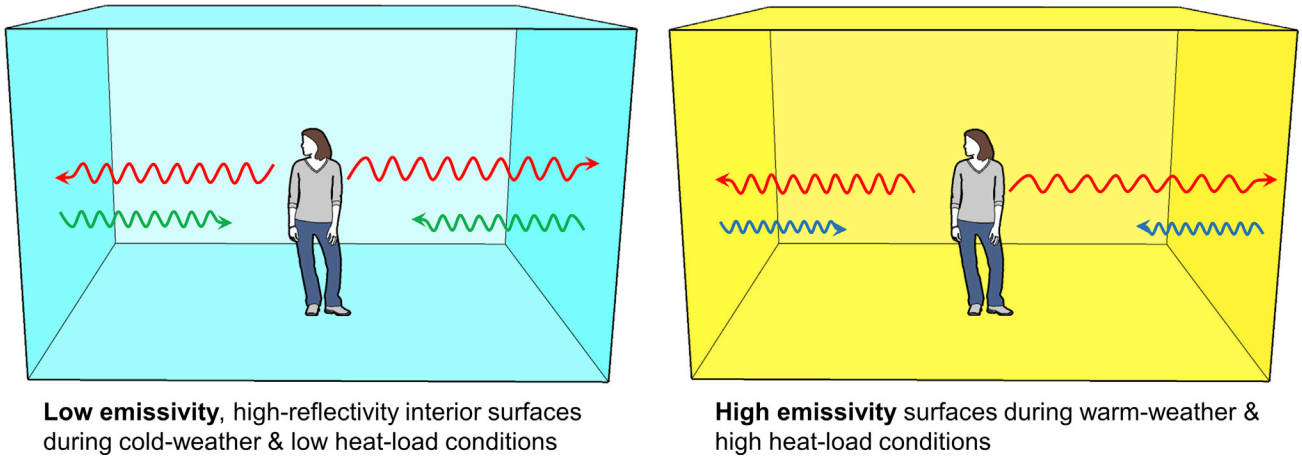

Figure 1. Conceptual schematic of tunable emissivity surfaces

Low-emissivity, high-reflectivity interior surface reflects radiative heat back to the body in cold weather conditions. By contrast, high-emissivity and absorptivity interior walls absorb the radiative heat released from the occupant during warm weather conditions

Minneapolis) and 33.5% (in Ancona) energy penalty relative to high-emissivity interior surfaces. Thus, tuning the interior surface's thermal emissivity enables maximal energy efficiency throughout the year, and in response to varying heat loads and conditions.

RESULTS AND DISCUSSION

The human body loses more than half of its heat through thermal radiation (Cai et al., 2017) in typical indoor environments. In cold weather conditions, finding a means to reduce this radiative heat loss in interior spaces is potentially an effective way to keep occupants comfortable at lower air temperatures than is typically maintained by heating. Most building materials, such as typical paints, wood, or brick have high emissivity (and therefore absorptivity) in the long-wave infrared. Thus, interior surfaces typically absorb the thermal radiation from the human occupant and emit back a smaller amount of thermal radiation corresponding to the lower temperature of the walls, ceilings, and floors. Our goal for cold weather conditions, schematically shown in Figure 1, is thus to have low-emissivity, high-reflectivity interior surfaces. By virtue of this property, the surfaces will send back a larger fraction of the radiative heat lost by the human occupant back to them, allowing us to set the air temperature lower, thereby reducing the need for heating energy while maintaining the same level of thermal comfort (which in our study is assessed by the maintenance of constant skin temperature and fixed amount of body heat released by the human occupant).

By contrast, in summer and warm weather conditions more generally, it is desirable to maximize the net heat rejected by the human occupant to their environment (Figure 1). Thus, high-emissivity (high-absorptivity) materials in the interior of the building should be used to absorb the heat radiated by the occupant. By doing so one can maintain the same level of thermal comfort while using less cooling energy than it would be needed if the walls were low emissivity or high reflectivity. This qualitative introduction to our concept highlights a key result of our analysis: the need for tunability in the emissivity of the surfaces surrounding the human occupant, depending on weather conditions and overall heat loads.

Set point change for the single occupant scenario

To numerically analyze the impact of emissivity on the interior air temperature set point, we developed a 3D computational model (Figure 2A) to simulate a standing person in a proto-typical conditioned space (see supplementary information Tables S1–S3 and Figures S1–S4 for details and validation of the numerical model by comparing our results with previously published experimental data). The room, whose dimensions are 3 m × 3 m × 3 m, has an air inlet where heating or cooling air is supplied and multiple outlets (shown in red) to ensure adequate distribution and flow of air in the space. The pathlines in Figure 2A indicate the heating/cooling air enters from the inlet and the calculated mean air velocity in the room is 0.11 m/s (see Figure S5 for temperature and velocity distribution at different planes). We simulated different scenarios with the wall temperatures of the room (including side walls, ceiling, and floor) ranging from 13°C to 25°C to represent conditions one typically encounters from cold to warm weather scenarios.

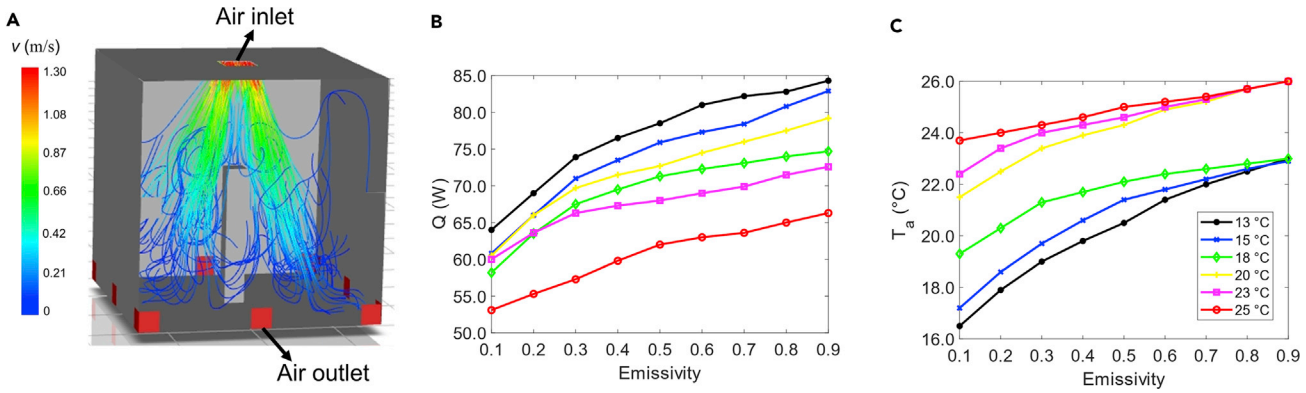

Figure 2. Computational model

(A): 3D model built to simulate a standing person in a conditioned space, to assess the impact of tuning the thermal emissivity of the spaces that surround the human occupant.

(B) Radiative heat loss of the occupant varies with the emissivity of their surroundings and is shown for six different wall temperature scenarios from 13°C to 25°C.

(C) The set point temperature varies as the emissivity of the interior surfaces surrounding the human occupant goes from 0.9 to 0.1

The non-sensible heat loss by the human occupants includes the heat loss by respiratory and evaporation from skin and is calculated at 50% relative air humidity for all scenarios (ANSI/ASHRAE, 2013). The metabolic rate of the standing adult in the room is 70W/m^2 (Cai et al., 2017). When the emissivity of the walls is 0.9, a fixed set point of 26°C in summer and 23°C in winter is applied to the six different wall temperature scenarios and the occupant's clothing insulation (enabled by the shell conduction function) is adjusted to have a skin temperature of 33°C (Oğulata, 2007; Takada et al., 2016). Then, the same clothing insulation is used throughout the same wall temperature scenario. As the emissivity of the interior wall changes, we adjust the air temperature to maintain a skin temperature of 33°C (with the same clothing insulation) to evaluate the effect of the emissivity on the set point. In the thermal comfort analysis section that follows, we also determine how the change in air temperature set point affects the human occupant's thermal comfort.

Figure 2B shows the total radiative heat loss from the human occupant to the environment. The radiation between the occupant and the interior is suppressed as the emissivity of the walls is decreased at six different wall temperatures. In cold weather, reducing the radiative heat transfer is beneficial for keeping the human warm while in warm weather it sabotages the occupant getting rid of the heat. The radiative heat loss can be reduced by 23.7% and 24.2%, respectively, at the wall temperature of 13°C and 15°C when the emissivity decreases from 0.9 to 0.1. In contrast, reducing the emissivity from 0.9 to 0.1 suppresses more than 14% of heat releasing radiatively in warm weather (when the wall temperature is equal to 23°C or 25°C) (see Figure S7 for radiative and convective heat loss).

Figure 2C shows the set point change as the emissivity of the interior varies in different wall temperature scenarios (for wall temperature coupled to external and internal environment scenario, see Figure S8 and see Figure S9 for the set point change results of an off-center positioned human occupant). We can see all the set point temperatures are at 26°C in summer and 23°C in winter when the emissivity is 0.9 in the six different wall temperature scenarios. As the emissivity starts to decrease, the set point must decrease to maintain the same skin temperature for the human occupant. The set point decreases when the emissivity is reduced because the occupant tends to lose less heat radiatively as shown in Figure 2B, thereby allowing for more heat loss convectively to colder air. When the wall temperature is set to 13°C, a decrease of set point as large as 6.5°C can be realized, which could yield meaningful energy savings (see the energy analysis session). In contrast when the weather is warm (wall temperatures at 23°C and 25°C), it is not favorable to have the emissivity of the walls low, because the cooling set point must be 3.6°C and 2.3°C lower, respectively, than it is when the emissivity of the walls is 0.9. These results highlight the need for tunability in the emissivity of interiors surrounding the occupant, depending on weather conditions.

A common trend we observed in Figures 2B and 2C is that the rate of change of both the radiative heat loss and set point temperature reduction accelerates when the emissivity approaches 0. To understand why, we

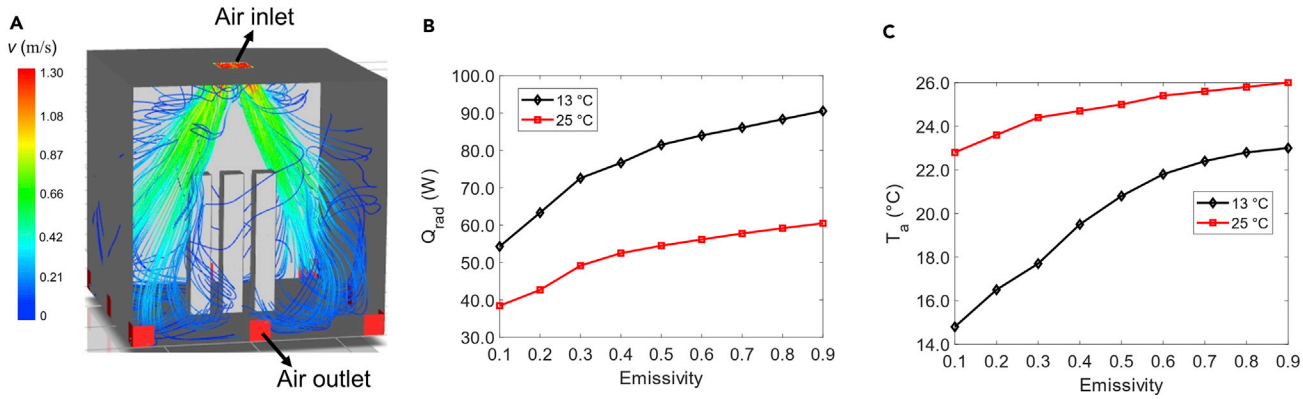

Figure 3. Multiple occupant scenario

(A) Computational model for multiple occupants in a conditioned space.

(B) Radiative heat loss as a function of emissivity in both cold weather (black line) and warm weather (red line) conditions

(C) The heating set point decreases from 23° to 14.8°C when the emissivity varies from 0.9 to 0.1 (black line), whereas the cooling set point increases from 22.8°C to 26°C as the emissivity increases from 0.1 to 0.9.

consider a simplified radiative heat transfer model for a human occupant and their surroundings that can be analytically evaluated. For a closed system consisting of two gray and diffuse surfaces, the radiative heat flux of the two surfaces can be analytically described as (Lienhard, 2011):

$$Q_{1,2} = \frac{(E_{b1} - E_{b2})}{\frac{1-\varepsilon_1}{\varepsilon_1 A_1} + \frac{1}{X_{1,2} A_1} + \frac{1-\varepsilon_2}{\varepsilon_2 A_2}} \quad \text{(Equation 1)}$$

In the above equations, $Q_{1,2}$ is the heat flux; A_1 is the area of the hot surface, in this case is the surface of the human cloth; A_2 is the sum of the cold surfaces area, in this case is the surface of the interiors; E_{b1} and E_{b2} are the black body emissions at the temperature of hot surface and cold surface, respectively, where $E_{b1} = \sigma T_1^4$, $E_{b2} = \sigma T_2^4$; σ is the Stephan-Boltzmann constant; T_1 is the hot surface temperature; T_2 is the cold surface temperature; ε_1 and ε_2 are the emissivity of the hot surface and the cold surface; X is the view factor.

When surface 1 is a plane or convex, Equation (2) can be simplified as (Lienhard, 2011):

$$Q = \frac{A_1 (E_{b1} - E_{b2})}{\frac{1}{\varepsilon_1} + \frac{A_1}{A_2}\left(\frac{1}{\varepsilon_2} - 1\right)} \quad \text{(Equation 2)}$$

Equation (2) can be used as a simplified way to calculate the radiative heat transfer between the occupant and their surroundings. From Equation (2), we can further see that when we decrease the emissivity of the cold surface the heat flux will be decreased as well. Equation (2) also shows that, as ε_2 approaches zero, the impact of the denominator increases sharply, agreeing with previous observations about the impact of emissivity (Robinson, 2016), which explains why we see an accelerated decrease of both radiative heat loss and set point temperature when the emissivity approaches 0.

Set point change for the multiple occupant scenario

Next, we investigated a common scenario in most buildings: the presence of more than one occupant in an interior space (Figure 3A), or more generically multiple heat sources. The pathlines in Figure 3A indicate that the heating/cooling air enters from the inlet and show that the mean air velocity in the room is 0.1 m/s (see Figure S6 for temperature and velocity distribution at different planes). We implemented this scenario numerically in both cold weather (wall temperature 13°C) and warm weather (wall temperature 25°C) scenarios. When there is more than one occupant in the same room, the heat source is effectively multiplied and there is heat transfer not only between occupant and surroundings but also between occupants. In typical cases, such as a classroom or movie theater, the space between different occupants is quite narrow. If we treat the multiple occupants a single, larger heat source, the emissivity effect will be enhanced according to Equation (2) because the area of the hot object increases. Extending this analysis when multiple occupants are in the same room, the low-emissivity walls will reflect not only their own heat back but also others' heat to them, which makes them feel warmer than the single occupant case. On the other hand,

in summer, if the walls reflect part of the radiative heat back, the multiple occupants will result in a significant cooling load for the air conditioner. However, if the walls can absorb most of the heat, the energy used in cooling will be substantially decreased.

The radiative heat flux and set point change resulting from varying emissivity in both winter and summer are shown in Figure 3. In the cold weather case, Figure 3B shows that the average radiative heat loss of each occupant decreases from 81.1W to 48.9W when the emissivity decreases from 0.9 to 0.1. There is also an acceleration of change after emissivity goes below 0.3. This leads to a sharp set point temperature decrease of 8.2°C when the emissivity is 0.1 (shown in Figure 3C). Similarly, in the warm weather case, the radiative heat loss of each occupant is increased from 38.4 W to 60.5 W when the emissivity increases from 0.1 to 0.9 (Figure 3B). There is also an acceleration in the heat transfer reduction as emissivity goes below 0.3. This leads to a sharp set point temperature decrease of up to 3.2°C when the emissivity is 0.1 (Figure 3C), necessitating substantially more cooling. These results highlight that, in dense spaces like classrooms, theaters, and indoor stadiums, a significant amount of energy can be saved by implementing a tunable emissivity surface on the walls, ceilings, and floors.

After obtaining the potential set point change as we vary the emissivity of the interiors at different wall temperatures, we next evaluated how this change could affect the thermal comfort level of the occupants.

Thermal comfort analysis

Thermal comfort is essential for human health, well-being, as well as productivity. A lack of thermal comfort can cause stress among occupants in a building (ASHRAE, 2013). Although thermal sensitivity varies from one person to another, six variables can be used to model a person's thermal comfort level: air temperature, mean radiant temperature, air velocity, air humidity, clothing resistance, and activity level (ASHRAE, 2013; Rupp et al., 2015). To qualitatively assess the thermal comfort level, the PMV model is the most widely used method in thermal comfort standards today (FANGER, 1970; Pourshaghaghy and Omidvari, 2012; Hasan et al., 2016). PMV is an index that aims to predict the mean value of votes of a group of occupants on a seven-point thermal sensation scale. Within the PMV index, +3, +2, +1 represent hot, warm, slightly warm, respectively, whereas −3, −2, −1 represent cold, cool, slightly cool, respectively. A PMV that falls between −0.5 and +0.5 is considered to represent the ideal thermal comfort status for a human being (Pourshaghaghy and Omidvari, 2012).

We adapt a thermal equilibrium approach to infer human thermal comfort (Pourshaghaghy and Omidvari, 2012; Hasan et al., 2016) for a range of emissivity conditions by computing the PMV:

$$PMV = \left(0.028 + 0.3033e^{-0.036M}\right) \times L \quad \text{(Equation 3)}$$

$$\begin{aligned} L = {} & (M-W) - 3.05\times10^{-3}(5733 - 6.99(M-W) - P_a) - 0.42(M-W-58.15) \\ & - 1.7\times10^{-5}(5867 - P_a) - 0.0014M(34 - t_a) - f_{cl}h_c(t_{cl} - t_a) \\ & - 3.96\times10^{-8}f_{cl}\left[(t_{cl}+273)^4 - (t_r+273)^4\right] \end{aligned} \quad \text{(Equation 4)}$$

Here L defines the overall heat transfer around an occupant in W/m^2, M is the metabolic rate in W/m^2, W is the work done by the occupant in W/m^2, P_a is the water vapor pressure in the air in Pa, t_r is the mean radiant temperature in °C, t_a is the air temperature in °C, f_{cl} is the clothing correction factor that accounts for the actual surface area of the clothed body compared with the body surface area, I_{cl} is the clothing insulation in clo, and h_c is the convective heat transfer coefficient in W/m^2.

Equation (4) is obtained by balancing the total heat transfer components for the human occupant of the conditioned space: (1) heat generation due to metabolism and the work done to the environment $(M-W)$, (2) convective heat transfer by $f_{cl}h_c(t_{cl} - t_a)$, (3) heat transfer through the skin $3.05\times10^{-3}(5733 - 6.99(M - W) - P_a)$, (4) heat transfer through latent respiration $1.7\times10^{-5}(5867 - P_a)$, (5) heat transfer by dry respiration $0.0014M(34 - t_a)$, and (6) heat transfer by radiation $3.96\times10^{-8}f_{cl}[(t_{cl}+273)^4 - (t_r+273)^4]$. In our evaluation, the relative humidity is set to 50% for all scenarios (ANSI/ASHRAE, 2013) (for different relative humidity PMV results, see Figure S10). The temperatures t_{cl} and t_a are obtained from our CFD calculation.

As shown in Equation (4), mean radiant temperature t_r is a key variable in thermal comfort for the human body. In prior work (Hensen, 1990; Pourshaghaghy and Omidvari, 2012; Yang et al., 2014; Rupp et al.,

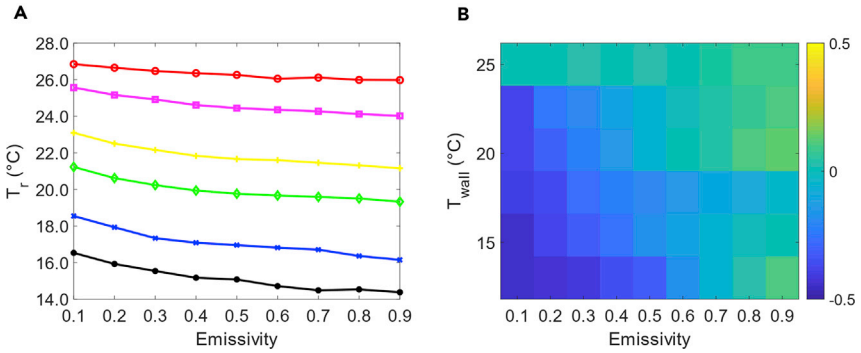

Figure 4. Thermal comfort evaluation

(A and B)(A) Mean radiant temperature t_r changes as the emissivity of the wall varies at different wall temperatures. (B) PMV for different wall temperatures with the emissivity of the building interiors varies from 0.9 to 0.1

2015; Hasan et al., 2016) and even in the ASHRAE standard 55 (ASHRAE, 2013), the mean radiant temperature is calculated based on an assumption that all the building materials have high emissivity (assumed to be ~1). Since in our analysis the emissivity of the building materials is changing dramatically, we must calculate the mean radiant temperature from its initial definitions:

$$Q_{rad} = \sigma\left(T_{cl}^4 - T_r^4\right) \quad \text{(Equation 5)}$$

$$T_r = \sqrt[4]{T_{cl}^4 - \frac{Q_{rad}}{\sigma}} \quad \text{(Equation 6)}$$

Here Q_{rad} is the radiative heat transferred between the occupant and the interior walls, which is obtained from the CFD calculation; T_r is the mean radiant temperature t_r in degrees Kelvin; T_{cl} is the temperature of the surface of clothing in degrees Kelvin. Figure 4A shows how the calculated mean radiant temperature t_r changes as the emissivity of the wall varies for different wall temperatures. We can see that t_r is increased as we decrease the emissivity of the wall. Since the surface temperature of the clothing is always higher than the wall temperature, t_r in all six different wall temperature scenarios is increased as the occupant loses less radiative heat to the surroundings (meaning that the occupant sees a warmer "object"). When the temperature difference between the surrounding walls and the surface of the clothing is larger in colder weather, the mean radiant temperature t_r increase is more significant (2.3°C when wall temperature is 13°C and 2.2°C when it is 15°C). However, when the wall temperature is closer to the clothing surface temperature the mean radiant temperature change t_r is less than 1°C.

From the above analysis, we obtained the thermal comfort index (PMV) for different wall temperatures with the emissivity of the building interior surfaces varying from 0.9 to 0.1. As shown in Figure 4B, the PMV remains in the −0.5 to +0.5 comfort zone. This result highlights that decreasing set point temperature in colder weather or increasing the set point in warm weather by changing the emissivity of the walls will not compromise the thermal comfort of the human occupants.

Energy savings analysis

To assess the building-level energy savings possible from our proposed approach, we use EnergyPlus, a widely used building energy analysis tool (Fumo et al., 2010). We use the changes in set point predicted by our CFD simulation results and apply them in EnergyPlus to estimate the energy savings for heating and cooling in a commercial building. For this preliminary analysis, we chose a small hotel reference building (*Commercial reference buildings. Available at: https://www.energy.gov/eere/buildings/commercial-reference-buildings.*, 2008) as our model building. The building has a low window/wall ratio (184.2 m^2/1,695 m^2), making it similar overall to the structure simulated in our CFD analysis (*Commercial reference buildings. Available at: https://www.energy.gov/eere/buildings/commercial-reference-buildings.*, 2008). We chose two locations, Ancona, Italy (Stazi et al., 2013), and Minneapolis, USA, to represent two types of climates with strong seasonal temperature variations: humid subtropical (also known as warm temperature) and continental climate, respectively. We first used the baseline set point previously mentioned (26°C in summer and 23°C in winter) to calculate the average internal surface wall temperature of all the guest rooms in this building. We then used the average internal surface temperature obtained from

Table 1. Average room internal surface temperature (°C), Minneapolis, USA

Jan	Feb	Mar	Apr	May	Jun	Jul	Aug	Sep	Oct	Nov	Dec
12.7	15.3	16.1	20.6	22.9	23.1	24.8	23.1	22.9	20.2	18.4	15.5

EnergyPlus and found the corresponding predicted set point change from our CFD calculations for that wall temperature. For example, if the average internal surface temperature is 18°C, we will use a 3.7°C set point decrease for heating, which is the value obtained according to the CFD calculation when the emissivity of interior surfaces is changed from 0.9 to 0.1.

Table 1 and Table 2 show the average internal surface wall temperature of all the guest rooms in the small hotel throughout the year in Minneapolis and Ancona, respectively. We then adjusted the set point used for each month according to the average wall temperature for that month and the corresponding CFD-based prediction for setpoint change. This then allows us to obtain a preliminary estimate of the whole year heating energy saving and cooling energy penalty for low-emissivity (0.1) surfaces in the two chosen locations.

Figure 5 shows the potential energy savings at the two locations throughout the year due to modified set points made possible by tuning the interior surface emissivity values to 0.1 during the heating season and 0.9 during the cooling season. We find that, in Figure 5, the energy used for heating in Minneapolis decreases from 379,930 to 242,539 kWh when we switch from a high-emissivity interior ($\varepsilon = 0.9$) to a low-emissivity interior ($\varepsilon = 0.1$), corresponding to a 36.8% savings in heating energy throughout a year. The heating energy consumption in Ancona decreases from 88,020 to 58,183 kWh when we use a low-emissivity interior ($\varepsilon = 0.1$), corresponding to 34.1%. Conversely, for cooling, the energy use in this hotel increases from 72,470 to 97,367 kWh when the emissivity changes from 0.9 to 0.1, which leads to a 34.7% energy penalty if the low-emissivity interior surfaces are not tuned back to high emissivity in Minneapolis during the cooling season. In Ancona, because of a longer cooling season, the cooling penalty due to low-emissivity surfaces is even larger with cooling energy consumption increasing from 104,845 to 139,996 kWh (a 33.5% energy penalty). Although this is a preliminary, first-order analysis of energy savings, we observe that the tunable emissivity of the internal surface in a building holds the potential to deliver significant energy savings. For more detailed modeling, EnergyPlus will need to be modified to accurately account for the effect of changing the long-wave infrared emissivity of interior surfaces on occupant thermal comfort, and thus the set point.

Conclusion

Our results indicate that tuning the emissivity of interior surfaces holds to the potential to deliver meaningful remarkable energy savings, particularly for heating. In recent years, a range of materials have shown the ability to tune their thermal emissivity (Mulford et al., 2019; Zhang et al., 2019b). Although these preliminary works indicate that tunable emissivity in the long-wave infrared part of the spectrum is in fact possible, our results highlight the need for further investigation of tunable emissivity materials that can meet the cost and performance targets suitable for large-area application in interior spaces. In the broader context of decarbonizing our built environment, the approach proposed and evaluated here represents a distinctive strategy that can complement a range of existing strategies, including radiant heating, and cooling, electrochromic windows and building integrated photovoltaics. Intriguing opportunities exist to combine the capabilities highlighted here with advances in smart building systems to develop interior spaces that dynamically respond to changing heat loads and occupants, to maximize both comfort and efficiency. More broadly, our results highlight an untapped degree of freedom for energy efficiency that lies in controlling the ubiquitous flows of heat that surround us every day.

Table 2. Average room internal surface temperature (°C), Ancona, Italy

Jan	Feb	Mar	Apr	May	Jun	Jul	Aug	Sep	Oct	Nov	Dec
18.2	18.7	19.6	21.2	22.0	23.2	24.1	24.3	23.7	22.1	20.4	19.2

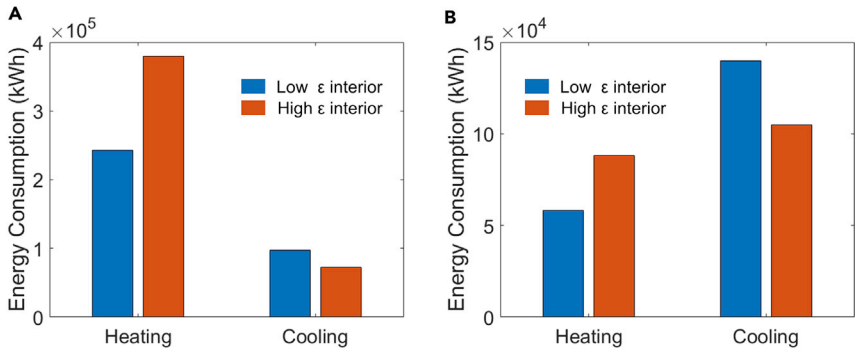

Figure 5. Potential energy savings throughout the year due to modified set points made possible by specific interior surface emissivity values

Annual energy use from a preliminary analysis for (A) heating and cooling by using high emissivity (ε = 0.9) and low-emissivity (ε = 0.1) interior in a small hotel reference building located in Minneapolis, USA (continental climate) and (B) in a small hotel reference building located in Ancona, Italy (humid subtropical climate).

Limitations of the study

This study presents and analyzes a mechanism for energy savings enabled by controlling the emissivity of the interior surfaces in a building. The analysis undertaken here is analytical and simulation-based and is thus a model of representative scenarios in the built environment. The actual impact on real-world building energy use will depend on the building's location, the climate, and the number of human occupants inside, necessitating experimental testing and validation.

STAR★METHODS

Detailed methods are provided in the online version of this paper and include the following:

- KEY RESOURCES TABLE
- RESOURCE AVAILABILITY
  - Lead contact
  - Materials availability
  - Data and code availability
- METHOD DETAILS
  - Computational fluid dynamics (CFD) modeling
  - Coupled wall temperature model
  - Validation of the CFD model
  - EnergyPlus modeling

SUPPLEMENTAL INFORMATION

Supplemental information can be found online at https://doi.org/10.1016/j.isci.2021.102825.

ACKNOWLEDGMENTS

A.R. acknowledges support of the UCLA Hellman Fellows Award and the Alfred P. Sloan Foundation (Sloan Research Fellowship in Physics).

AUTHOR CONTRIBUTIONS

Conceptualization, A.P.R.; methodology, J.X. and A.P.R; software, J.X.; formal analysis, J.X. and A.P.R., investigation, J.X. and A.P.R.; writing – original draft, J.X. and A.P.R.; writing – review & editing, J.X. and A.P.R.; visualization, J.X.; supervision, A.P.R.

DECLARATION OF INTERESTS

The authors declare no competing interests.

Received: December 31, 2020
Revised: April 13, 2021
Accepted: June 29, 2021
Published: August 20, 2021

REFERENCES

ANSI/ASHRAE (2013). Thermal Environmental Conditions for Human Occupancy Standard 55-2013, *55* (Ashrae ASHRAE Standard).

Zhou, H., Zhang, T., Yue, X., Peng, Y., Qiu, F., and Yang, D. (2019). Fabrication of flexible and superhydrophobic melamine sponge with aligned copper nanoparticle coating for self-cleaning and dual thermal management properties. Ind. Eng. Chem. Res. *58*, 4844–4852.

ANSI/ASHRAE (2017) ASHRAE Handbook—Fundamentals.

Arslanoglu, N., and Yigit, A. (2016). Experimental and theoretical investigation of the effect of radiation heat flux on human thermal comfort. Energy Buildings *113*, 23–29.

ASHRAE, A.H. (2013) 'Fundamentals, SI ed., American Society of Heating Refrigeration and Air-Conditioning Engineers', Inc., USA.

Brooke, R., Mitraka, E., Sardar, S., Sandberg, M., Sawatdee, A., Berggren, M., Crispin, X., and Jonsson, M.P. (2017). Infrared electrochromic conducting polymer devices. J. Mater. Chem. C *5*, 5824–5830.

Cai, L., Peng, Y., Xu, J., Zhou, Chenyu, Zhou, Chenxing, Wu, P., Lin, D., Fan, S., and Cui, Y. (2019). Temperature regulation in colored infrared-transparent polyethylene textiles. Joule *3*, 1478–1486.

Cai, L., Song, A.Y., Wu, P., Hsu, P.-C., Peng, Y., Chen, J., Liu, C., Catrysse, P.B., Liu, Y., Yang, A., et al. (2017). Warming up human body by nanoporous metallized polyethylene textile. Nat. Commun. *8*, 496. https://doi.org/10.1038/s41467-017-00614-4.

Chafi, F.Z., and Hallé, S. (2011). Three dimensional study for evaluating of air flow movements and thermal comfort in a model room: experimental validation. Energy Buildings *43*, 2156–2166.

Cheng, Y., Niu, J., Liu, X., and Gao, N. (2013). Experimental and numerical investigations on stratified air distribution systems with special configuration: thermal comfort and energy saving. Energy Buildings *64*, 154–161.

Coutts, A.M., White, E.C., Tapper, N.J., Beringer, J., and Livesley, S.J. (2016). Temperature and human thermal comfort effects of street trees across three contrasting street canyon environments. Theor. Appl. Climatol. *124*, 55–68. https://doi.org/10.1007/s00704-015-1409-y.

Defraeye, T., Blocken, B., and Carmeliet, J. (2011). Convective heat transfer coefficients for exterior building surfaces: existing correlations and CFD modelling. Energy Convers. Management *52*, 512–522.

Dickson, T., and Pavía, S. (2021). Energy performance, environmental impact and cost of a range of insulation materials. Renew. Sustain. Energy Rev. *140*, 110752.

FANGER, P.O. (1970). Thermal Comfort. Analysis and Applications in Environmental Engineering (Danish Technical Press).

Fumo, N., Mago, P., and Luck, R. (2010). Methodology to estimate building energy consumption using EnergyPlus Benchmark Models. Energy and Buildings *42*, 2331–2337.

Guo, Y., Li, K., Hou, C., Li, Y., Zhang, Q., and Wang, H. (2016). Fluoroalkylsilane-modified textile-based personal energy management device for multifunctional wearable applications. ACS Appl. Mater. Interfaces *8*, 4676–4683. https://doi.org/10.1021/acsami.5b11622.

Hasan, M.H., Alsaleem, F., and Rafaie, M. (2016). Sensitivity study for the PMV thermal comfort model and the use of wearable devices biometric data for metabolic rate estimation. Building Environ. *110*, 173–183.

Hensen, J.L.M. (1990). Literature review on thermal comfort in transient conditions. Building Environ. *25*, 309–316.

Hoyt, T., Lee, K.H., Zhang, H., Arens, E. and Webster, T. (2005) Energy Savings from Extended Air Temperature Setpoints and Reductions in Room Air Mixing.

Hsu, P.-C., Liu, X., Liu, C., Xie, X., Lee, H.R., Welch, A.J., Zhao, T., and Cui, Y. (2015). Personal thermal management by metallic nanowire-coated textile. Nano Letters *15*, 365–371. https://doi.org/10.1021/nl5036572.

Hsu, P.-C., Song, A.Y., Catrysse, P.B., Liu, C., Peng, Y., Xie, J., Fan, S., and Cui, Y. (2016). Radiative human body cooling by nanoporous polyethylene textile. Science *353*, 1019 LP–1023. http://science.sciencemag.org/content/353/6303/1019.abstract.

Kant, K., Shukla, A., Sharma, Atul, and Sharma, A. (2018). Advances in Simulation Studies for Developing Energy-Efficient Buildings (CRC Press), pp. 209–233.

Kingma, B., and van Marken Lichtenbelt, W. (2015). Energy consumption in buildings and female thermal demand. Nat. Clim. Change *5* (12), 1054–1056.

Lienhard, J.H. (2011). A Heat Transfer Textbook, 2011th edn (Courier Corporation).

Liu, W., Lian, Z., Deng, Q., and Liu, Y. (2011). Evaluation of calculation methods of mean skin temperature for use in thermal comfort study. Building Environ. *46*, 478–488.

Liu, Y., Wang, L., Liu, J., and Di, Y. (2013). A study of human skin and surface temperatures in stable and unstable thermal environments. J. Therm. Biol. *38*, 440–448.

Moon, J.H., Lee, J.W., Jeong, C.H., and Lee, S.H. (2016). Thermal comfort analysis in a passenger compartment considering the solar radiation effect. Int. J. Therm. Sci. *107*, 77–88.

Mulford, R.B., Dwivedi, V.H., Jones, M.R., and Iverson, B.D. (2019). Control of net radiative heat transfer with a variable-emissivity accordion tessellation. J. Heat Transfer *141*, 32702.

Oğulata, R.T. (2007). The effect of thermal insulation of clothing on human thermal comfort. Fibres Textiles East. Europe *15*, 61.

Okamoto, T., Tamura, K., Miyamoto, N., Tanaka, S., and Futaeda, T. (2017). Physiological activity in calm thermal indoor environments. Sci. Rep. *7*, 11519. https://doi.org/10.1038/s41598-017-11755-3.

Pérez-Lombard, L., Ortiz, J., and Pout, C. (2008). A review on buildings energy consumption information. Energy Buildings *40*, 394–398. https://doi.org/10.1016/j.enbuild.2007.03.007.

Pourshaghaghy, A., and Omidvari, M. (2012). Examination of thermal comfort in a hospital using PMV–PPD model. Appl. Ergon. *43*, 1089–1095.

Qiu, Q., Zhu, M., Li, Z., Qiu, K., Liu, X., Yu, J., and Ding, B. (2019). Highly flexible, breathable, tailorable and washable power generation fabrics for wearable electronics. Nano Energy *58*, 750–758.

Robinson, A.J. (2016). A thermal model for energy loss through walls behind radiators. Energy Buildings *127*, 370–381.

Rupp, R.F., Vásquez, N.G., and Lamberts, R. (2015). A review of human thermal comfort in the built environment. Energy Buildings *105*, 178–205. https://doi.org/10.1016/j.enbuild.2015.07.047.

Schiavoni, S., Bianchi, F., and Asdrubali, F. (2016). Insulation materials for the building sector: a review and comparative analysis. Renew. Sustain. Energy Rev. *62*, 988–1011.

Shen, P., Dai, M., Xu, P., and Dong, W. (2019). Building heating and cooling load under different neighbourhood forms: assessing the effect of external convective heat transfer. Energy *173*, 75–91.

Stazi, F., Vegliò, A., Di Perna, C., and Munafò, P. (2013). Experimental comparison between 3 different traditional wall constructions and dynamic simulations to identify optimal thermal insulation strategies. Energy Buildings *60*, 429–441. https://doi.org/10.1016/j.enbuild.2013.01.032.

Takada, S., Sasaki, A., and Kimura, R. (2016). Fundamental study of ventilation in air layer in clothing considering real shape of the human

body based on CFD analysis. Building Environ. *99*, 210–220.

Teitelbaum, E., Chen, K.W., Aviv, D., Bradford, K., Ruefenacht, L., Sheppard, D., Teitelbaum, M., Meggers, F., Pantelic, J., and Rysanek, A. (2020). Membrane-assisted radiant cooling for expanding thermal comfort zones globally without air conditioning. Proc. Natl. Acad. Sci. *117*, 21162–21169.

The heat is on. Nat. Energy *1*, 16193. https://doi.org/10.1038/nenergy.2016.193.

Tong, J.K., Huang, X., Boriskina, S.V., Loomis, J., Xu, Y., and Chen, G. (2015). Infrared-transparent visible-opaque fabrics for wearable personal thermal management. ACS Photon. *2*, 769–778. https://doi.org/10.1021/acsphotonics.5b00140.

Ürge-Vorsatz, D., Cabeza, L.F., Serrano, S., Barreneche, C., and Petrichenko, K. (2015). Heating and cooling energy trends and drivers in buildings. Renew. Sustain. Energy Rev. *41*, 85–98.

Wang, H., Chiang, P.-C., Cai, Y., Li, C., Wang, X., Chen, T.-L., Wei, S., and Huang, Q. (2018). Application of wall and insulation materials on Green building: a review. Sustainability *10*, 3331.

Wijeysundera, N.E. (2015). Principles of Heating, Ventilation and Air Conditioning with Worked Examples (World Scientific).

Winslow, C.-E., Gagge, Ap., and Herrington, L.P. (1939). The influence of air movement upon heat losses from the clothed human body. Am. J. Physiol. Legacy Content *127*, 505–518.

Xu, J.W., Toppare, L., Li, Y., Xu, C., Kim, E., Zhong, Y.-W., Zhang, C., Beneduci, A., Ak, M., and Hsiaob, S.-H. (2019). Electrochromic Smart Materials: Fabrication and Applications (Royal Society of Chemistry).

Yang, L., Yan, H., and Lam, J.C. (2014). 'Thermal comfort and building energy consumption implications – a review'. Appl. Energy *115*, 164–173. https://doi.org/10.1016/j.apenergy.2013.10.062.

Yu, Y., Megri, A.C., and Jiang, S. (2019). A review of the development of airflow models used in building load calculation and energy simulation. In Building Simulation (Springer), pp. 347–363.

Yue, X., Zhang, T., Yang, D., Qiu, F., Li, Z., Wei, G., and Qiao, Y. (2019). Ag nanoparticles coated cellulose membrane with high infrared reflection, breathability and antibacterial property for human thermal insulation. J. Colloid Interface Sci. *535*, 363–370. https://doi.org/10.1016/j.jcis.2018.10.009.

Zhang, L., Wang, B., Li, X., Xu, G., Dou, S., Zhang, X., Chen, X., Zhao, J., Zhang, K., and Li, Y. (2019a). Further understanding of the mechanisms of electrochromic devices with variable infrared emissivity based on polyaniline conducting polymers. J. Mater. Chem. C *7*, 9878–9891.

Zhang, X., Tian, Y., Li, W., Dou, S., Wang, L., Qu, H., Zhao, J., and Li, Y. (2019b). Preparation and performances of all-solid-state variable infrared emittance devices based on amorphous and crystalline WO3 electrochromic thin films. Solar Energy Mater. Solar Cells *200*, 109916.

STAR★METHODS

KEY RESOURCES TABLE

REAGENT or RESOURCE	SOURCE	IDENTIFIER
Software and algorithms		
Ansys Fluent	ANSYS, Inc	https://www.ansys.com/
EnergyPlus	U.S. Department of Energy's (DOE) Building Technologies Office (BTO), and National Renewable Energy Laboratory (NREL)	https://energyplus.net/

RESOURCE AVAILABILITY

Lead contact

Further information requests should be directed to the lead contact, Professor Aaswath Raman (aaswath@ucla.edu).

Materials availability

This study did not generate new reagents.

Data and code availability

All data and analytical methods are reported in the main text or in the supplementary information section.

METHOD DETAILS

Computational fluid dynamics (CFD) modeling

ANSYS workbench mesh (v19.0) is used to generate the hexahedral dominated cutcell mesh for the whole domain, with a total number of 245284. The simulations are performed using ANSYS Fluent (v19.0). Steady state simulations for incompressible flows are implemented. The realizable k-ε model with standard wall functions is adopted to deal with turbulence. The DO (discrete ordinates) radiation model is used to calculate radiative heat transfer between the occupants and the wall, and the SIMPLE algorithm is adopted to deal with the coupling of the pressure and the velocity. The discretization of the convection term in all equations is the second order upwind scheme and for the diffusion term, the second order central scheme is used. We maintain the constant temperature of the occupants' skin and fixed heat released from them by changing the set point temperature of the room.

Coupled wall temperature model

In practice, the wall temperature can change due to indoor air temperature variation. We assume an outside air temperature of 5°C in winter and 27°C in summer and the wall temperature is both determined by the external and internal environment (walls have the thickness of 0.37m and the conductivity of 0.77W/(m·K) (Defraeye et al., 2011; Wijeysundera, 2015) and the external surfaces have a mixed boundary taking both convection (heat transfer coefficient of 21.6W/(m^2·K) (Wijeysundera, 2015) and free stream temperature of 5°C and 27°C respectively) and radiation (radiation temperature of 5°C and 27°C respectively and external emissivity of 0.9) into consideration as schematically shown in Figure S3 (a)). We can see in winter as the indoor temperature decreases, the interior wall temperature also decreases from 14.4°C to 12.3°C (2.1°C drop in winter as the emissivity varies), the set point change in winter can reach 3.6°C when the emissivity of the wall changes to 0.1 from 0.9. 3.6°C is a smaller change compared with our initial calculation which is meant to be a guidance of the highest potential set point change. However, a 3.6°C set point change is still meaningful in terms of building energy saving. In summer, the temperature change is smaller due to the smaller difference between indoor and outdoor temperature.

Validation of the CFD model

We validate the numerical method implemented in this paper by comparing its results against experimental data previously. In their analysis, Chafi and Hallé built a model room equipped with ventilation system in the laboratory (Chafi and Hallé, 2011). The room measures 4.88 m × 3.66 m and has a height of 3 m.

Constant wall temperatures are maintained by flowing warm or cold through them in the experiment. There are 21 thermocouples installed in different horizon planes of 0.1m, 0.6m, 1.1m, 1,7m and 2.3m. The geometry of the model room is shown in Figure S2. All the boundary conditions in our numerical simulation are corresponding to the measurement data. The boundary conditions are shown in the Table S3.

Figure S3 shows the comparison between the experimental measurements and the CFD results in different positions. While there are measurable differences between the measurements and CFD predictions, they are below 5.3% at all positions. In summary, the numerical prediction from our CFD model agrees reasonably well with the published experimental measurements.

EnergyPlus modeling

EnergyPlus (v7-2-0) is implemented to assess the total energy saving in a reference building meant to represent a small hotel. "HTGSETP_SCH" and "CLGSETP_SCH", which are the heating and cooling set point schedule respectively, are changed according to the CFD calculation results.